Theory of Proton Hyperfine Interaction in High-Spin Five- and Six-Liganded Iron and Manganese Heme Systems†

S. K. Mun, Mahendra K. Mallick, Shantilata Mishra, Jane C. Chang, and T. P. Das*

Contribution from the Department of Physics, State University of New York at Albany, Albany, New York 12222. *Received March 6, 1981*

Abstract: Proton hyperfine interactions provide valuable information regarding the nature of the unpaired spin population distributions over the peripheral regions of the heme unit of hemoglobin derivatives. With this feature in mind we have analyzed the contributions to the hyperfine interactions of protons in a number of high-spin five-liganded (F–, Cl–, Br–, I–, and OH–FeP) and six-liganded (Met– and F–Mb, H_2O–Mn and Cl–$Mn^{III}P$) heme compounds, data on the hyperfine interactions for a number of these protons being available from ENDOR measurements. Unpaired spin populations over the atoms, obtained from self-consistent-charge extended Hückel calculations, which have been shown from earlier work on ^{57}Fe, ^{14}N, and halogen nuclear hyperfine interactions to provide a satisfactory description of the spin distributions in the central regions of a number of the molecules studied, are also utilized in the present investigations. Our results show that the electron-nuclear magnetic dipolar interactions make a major contribution to the hyperfine fields at the protons in high-spin heme and hemoglobin systems, and that it is important to consider the actual unpaired spin population–distribution over the entire molecule in question instead of making an approximation of taking all the unpaired spin population as localized on the central metal atom. It is also shown that while the direct and exchange contact contributions are both smaller than the dipolar contributions, they do have important influence on the net hyperfine constants. For those cases where experimental results are available, satisfactory agreement is obtained for both the observed magnitudes and trends of the proton hyperfine constants.

I. Introduction

A number of experimental techniques, among them, electron spin resonance[1] (ESR), nuclear magnetic resonance[2] (NMR), electron nuclear double resonance[3] (ENDOR), and Mössbauer spectroscopy,[4] have been used to provide valuable information about the electronic structures of hemin and hemoglobin derivatives, by the study of the magnetic hyperfine interaction at the hydrogen, iron, nitrogen, carbon, fluorine, chlorine, and bromine nuclear sites in these molecules. In earlier work,[5,6] we have studied the ^{57}Fe, ^{55}Mn, and ^{14}N magnetic hyperfine interactions in a series of five-ligand high-spin hemins, namely, fluoro-, chloro-, bromo-, and hydroxyferric porphyrins (abbreviated as F–, Cl–, Br–, and OH–FeP, respectively), divalent and trivalent manganese porphyrins with H_2O and Cl as fifth ligands (abbreviated as H_2O–$Mn^{II}P$ and Cl–$Mn^{III}P$, respectively), and two six-liganded high-spin systems, metmyoglobin and fluoromyoglobin derivatives (abbreviated as Met– and F–Mb, respectively). These studies[5,6] have analyzed the electronic distributions mainly in the central regions of the porphyrin and histidine (in F–Mb and Met–Mb), referring to the vicinity of the metal atom and its immediate ligands. The present work is intended to provide additional information on the electronic structures in those molecules by the study of the magnetic hyperfine interactions of protons at the peripheral regions of the porphyrins (i.e., meso protons) as well as in other peripheral regions of the molecule. We also include a high-spin five-liganded hemin derivative, namely, iodohemin (I–FeP) in the present study.

A knowledge of the electron distribution in the peripheral regions of all these five- and six-liganded heme systems is expected to be important for the understanding of two biological processes, namely, electron-tunnelling[7] in the related cytochrome systems and the exchange of information between the heme system and the protein associated with the conformational changes important for the cooperative oxygenation process.

A large number of ^1H shifts[7,8] both in the high- and low-spin hemins and in the hemoglobin derivatives are available from NMR measurements. The analysis of these proton shifts requires the knowledge[9] of the susceptibility tensor in addition to the hyperfine coupling constants of the proton. On the other hand, ENDOR data on the magnetic hyperfine splitting of spin levels of protons[10] directly provide the proton hyperfine coupling constants. ENDOR data are available[11] on a limited number of protons, namely, the meso protons, heme-bound water protons, and some of the imidazole protons in the hemin and hemoglobin systems.

In the present work we shall concentrate our attention on the interpretation of the available proton ENDOR data[11] in terms of the electronic wave functions we have obtained for our earlier work on ^{57}Fe and ^{14}N hyperfine interactions. The side chains on the pyrroles were replaced by hydrogen atoms to reduce the computational effort. In future work, we hope to include the side chains on the pyrroles where a number of the protons for which NMR shift data are available[2] are located. In the present work we shall concentrate on the proton hyperfine constants which are available from ENDOR measurements.

Recent ENDOR studies[11] on the five-ligand high-spin hemins show that the meso-proton hyperfine coupling constant (about 1.0 MHz) varies very little from one halogen derivative to the other. Moreover, it is observed that this coupling constant for the six-ligand Met–Mb and F–Mb is somewhat smaller in mag-

†Supported by Grant HL15196 from the Heart, Blood, and Lung Institute of the National Institutes of Health.

*Author to whom inquiries should be addressed at Department of Physics, State University of New York at Albany, Albany, NY, 12222.

(1) See, for example, (a) M. Chevion, A. Stern, J. Peisach, W. E. Blumberg, and S. Simon, *Biochemistry*, **17**, 1745 (1978); (b) J. C. W. Chien and L. C. Dickinson, *J. Biol. Chem.*, **252**, 1331 (1977); (c) T. Yonetani, H. Yamamoto, J. E. Erman, J. S. Leigh, Jr., and G. H. Reed, *ibid.*, **247**, 2447 (1972).

(2) See, for example, (a) G. N. LaMar, M. Overkamp, H. Sick, and K. Gersonde, *Biochemistry*, **17**, 352 (1978); (b) M. E. Johnson, L. W.-M. Fun, and C. Ho, *J. Am. Chem. Soc.*, **99**, 1245 (1977); (c) R. G. Shulman, S. H. Glarum, and M. Karplus, *J. Mol. Biol.*, **57**, 93 (1971).

(3) See, for example, (a) C. P. Scholes, R. A. Isaacson, T. Yonetani, and G. Feher, *Biochim. Biophys. Acta*, **322**, 457 (1973); (b) G. Feher, R. A. Isaacson, C. P. Scholes, and R. L. Nagel, *Ann. N.Y. Acad. Sci.*, **222**, 86 (1973).

(4) See, for example, (a) G. Lang and W. Marshall, *Proc. Phys. Soc. London*, **81**, 3 (1966); (b) C. E. Johnson, *Phys. Lett.*, **21**, 491 (1966).

(5) M. K. Mallick, J. C. Chang, and T. P. Das, *J. Chem. Phys.*, **68**, 1462 (1978).

(6) (a) S. K. Mun, J. C. Chang, and T. P. Das, *Biochim. Biophys. Acta*, **490**, 249 (1977); (b) M. K. Mallick, S. K. Mun, S. Mishra, J. C. Chang, and T. P. Das, *Hyperfine Interact.*, **4**, 914 (1978).

(7) J. J. Hopfield, *Proc. Natl. Acad. Sci. U.S.A.*, **71**, 3640 (1974).

(8) (a) R. J. Kurland, R. G. Little, D. G. Davis, and C. Ho, *Biochemistry*, **10**, 2237 (1971); (b) F. A. Walker and G. N. LaMar, *Ann. N.Y. Acad. Sci.*, **206**, 328 (1973); (c) G. N. LaMar, G. R. Eaton, R. H. Holm, and F. A. Walker, *J. Am. Chem. Soc.*, **95**, 63 (1973).

(9) H. M. McConnell, *J. Chem. Phys.*, **24**, 764 (1956).

(10) H. L. Van Camp, C. P. Scholes, C. F. Mulks, and W. S. Caughey, *J. Am. Chem. Soc.*, **99**, 8383 (1977).

(11) C. F. Mulks, C. P. Scholes, L. C. Dickinson, and A. Lapidot, *J. Am. Chem. Soc.*, **101**, 1645 (1979).

0002-7863/81/1503-5024$01.25/0

nitude (about 0.8 MHz) compared to that for the five-ligand hemins. A large proton hyperfine splitting of about 6.0 MHz that is observed in the ENDOR measurements in Met–Mb and Met–Hb has been assigned[11] to the heme-bound H_2O proton. Hyperfine coupling constants of the protons in the imidazole of the proximal histidine have also been reported from ENDOR measurements. In our present work, we shall investigate the contributions from the different mechanisms[5,6,12,13] that produce the proton hyperfine interaction, namely, the direct contact interaction, the exchange polarization interaction, and the magnetic dipolar interaction. The investigations of these different mechanisms will be carried out both to attempt to explain the observed proton hyperfine constants and to obtain insight into the relative importance of the various contributing mechanisms. We also hope from our investigations to obtain useful information on the effect on the spin distribution and the proton hyperfine interaction when divalent and trivalent manganese replace the iron atom in the five-liganded heme system.

II. Procedure

The magnetic hyperfine interactions at the proton sites can arise from several mechanisms.[12,13] The first is the dipolar interaction between the proton magnetic moment and the delocalized unpaired electron spin distribution over the molecule. The second is the direct contact interaction of the spin density at the proton site with the proton magnetic moment. The third contribution comes from the exchange polarization effect[14,15] between the electrons in the bond between the hydrogen atom and the adjacent atom (such as the meso carbon in the case of meso proton) and the unpaired spin distribution on the adjacent atom. To obtain the spin distributions and the unpaired electron densities at the nuclei, one requires the electronic wave functions for the molecule. The electronic wave functions for F–, Cl–, Br–, and OH–FeP, H_2O–$Mn^{II}P$, Cl–$Mn^{III}P$, F–Mb, and Met–Mb, which were determined previously,[5,6] using the self-consistent-charge extended Hückel (SCCEH) procedure[16,17] were used for the present work. In the case of I–FeP, the SCCEH procedure was also used to obtain the electronic wave functions, the geometry of the porphyrin ring being taken to be the same as that in the other halogen derivatives[5] with iodine atom on the Z axis and the Fe–I distance being chosen as 2.56 Å from the differences in the bond radii between iodine and other halogen atoms.[18]

In the SCCEH procedure,[16,17] the molecular orbitals (MO) ϕ_μ are expressed as a linear combination of atomic orbitals (AO) χ_i

$$\phi_\mu = \sum_i C_{\mu i}\chi_i \tag{1}$$

where $C_{\mu i}$'s are LCAO coefficients and the summation is carried over all the valence orbitals of every atom in the molecule. The valence orbitals used were the 3d, 4s, and 4p AO's of iron and manganese, 2s and 2p AO's of carbon, nitrogen, oxygen, and fluorine, 3s and 3p AO's of chlorine, 4s and 4p AO's of bromine, and 5s and 5p AO's of iodine. A detailed description of the theoretical procedure we have used for obtaining the LCAO coefficients $C_{\mu i}$ is available in the literature and in some of our earlier publications[5,17,19] on hyperfine and magnetic properties of heme compounds.

Table I. Unpaired Spin Populations on Atoms of Five Liganded Systems

atoms	Fe–FeP	Cl–FeP	Br–FeP	I–FeP	OH–FeP
Fe	3.122	3.240	3.196	3.173	3.096
N_2	0.258	0.245	0.222	0.209	0.214
C_6	0.023	0.017	0.014	0.012	0.013
C_7	0.018	0.014	0.012	0.010	0.011
C_8	0.037	0.034	0.026	0.025	0.028
H_{26}	0.0	0.0	0.0	0.0	0.0
H_{27}	0.001	0.001	0.001	0.001	0.001
R_{38}[a]	0.365	0.388	0.600	0.709	0.722
R_{39}[b]					0.0157

[a] R_{38} represents F, Cl, Br, I and O in F–, Cl–, Br–, I–, and OH–FeP respectively. [b] R_{39} in OH–FeP represents the OH hydrogen.

Table II. Unpaired Spin Populations on Atoms of Maganese Prophyrins

atom	H_2O–$Mn^{II}P$	Cl–$Mn^{II}P$[a]
Mn	3.574	2.868
N_2	0.192	0.089
C_6	0.022	0.017
C_7	0.023	0.016
C_8	0.019	0.019
C_{11}	0.021	-
C_{12}	0.024	-
C_{13}	0.020	-
H_{26}	0.000	0.000
H_{27}	0.001	0.001
H_{29}	0.000	-
H_{30}	0.001	-
R_{38}[b]	0.207	0.426
R_{39}[c]	0.004	

[a] Spaces marked "-" indicate equivalent atoms. [b] R_{38} represents the oxygen and chlorine atom in H_2O–$Mn^{II}P$ and Cl–Cl–$Mn^{III}P$, respectively. [c] R_{39} represents one of the hydrogen atoms in H_2O of H_2O–$Mn^{II}P$.

The unpaired electronic population ρ_i for χ_i, using the MO functions in χ_i, 1, is given by[19,20]

$$\rho_i = q_i^\alpha - q_i^\beta \tag{2}$$

with

$$q_i^\alpha = \sum_\mu \{(C_i^\alpha)^2 + \sum_{j>i} C_{\mu i}^\alpha C_{\mu j}^\alpha S_{ij}\} n_\mu^\alpha \tag{3}$$

$$q_i^\beta = \sum_\mu \{(C_{\mu i}^\beta)^2 + \sum_{j>i} C_{\mu i}^\beta C_{\mu j}^\beta S_{ij}\} n_\mu^\beta \tag{4}$$

$$S_{ij} = \langle \chi_i | \chi_j \rangle \tag{5}$$

where q_i^α and q_i^β are the electronic populations in the AO, χ_i, corresponding to the majority and minority spin states α and β, respectively. The symbol n_μ^α represents the number of electrons in the MO ϕ_μ^α, and S_{ij} is the overlap integral between the AO's χ_i and χ_j. The unpaired electronic population on an atom can be obtained by summing ρ_i over all the valence AO's of the atom. Before proceeding to study the magnetic hyperfine interaction of the protons, we would like to present a few features of the unpaired electronic populations in the molecules under study. The point group for the models we have used for the molecules F–, Cl–, Br–, I–, and OH–FeP and Cl–$Mn^{III}P$ is C_{4v}, and for H_2O–$Mn^{II}P$ it is C_{2v}. In Tables I and II, we present the unpaired electronic populations on the inequivalent atoms in the five-ligand iron and manganese porphyrins, respectively. Since there is no symmetry in F–Mb and Met–Mb we present the unpaired electronic population on all atoms in these six-liganded molecules in Table III. One notable feature observed from Tables I and III is that about 35 to 40% of the total unpaired spin electron population has been distributed over the ligand atoms in the five- and six-liganded

(12) T. P. Das, "Relativistic Quantum Theory of Electronics", Harper and Row, New York 1973, Chapter 7, and references therein.
(13) J. E. Wertz and J. R. Bolton, "Electron Paramagnetic Resonance", McGraw-Hill, New York 1972.
(14) H. M. McConnell, *Proc. Natl. Acad. Sci. U.S.A.*, **69**, 335 (1972).
(15) (a) J. E. Rodgers, T. Lee, T. P. Das, and D. Ikenberry, *Phys. Rev. A*, **7**, 51 (1973); (b) J. E. Rodgers and T. P. Das, *ibid.*, **8**, 2195 (1973).
(16) M. Zerner, M. Gouterman, and H. Kobayashi, *Theor. Chim. Acta*, **6**, 363 (1966).
(17) P. S. Han, T. P. Das, and M. F. Rettig, *J. Chem. Phys.*, **56**, 3861 (1972).
(18) L. Pauling, "The Nature of the Chemical Bond", 2nd ed., Cornell University, Ithaca, N.Y., 1948, p 164.
(19) J. C. Chang, Y. M. Kim, T. P. Das, and K. J. Duff, *Theor. Chim. Acta*, **41**, 37 (1976).
(20) R. S. Mulliken, *J. Chem. Phys.*, **23**, 1833 (1955).

Table III. Unpaired Electronic Population on Atoms in Met-Mb and F-Mb

atom	Met-Mb	F-Mb	atom	Met-Mb	F-Mb	atom	Met-Mb	F-Mb
Fe	3.165	3.046	C_{21}	0.025	0.031	N_ϵ	0.259	0.160
N_2	0.205	0.234	C_{22}	0.016	0.022	C_a	0.011	0.008
N_3	0.201	0.243	C_{23}	0.011	0.012	C_b	0.043	0.012
N_4	0.206	0.243	C_{24}	0.016	0.022	N_δ	0.165	0.010
N_5	0.205	0.233	C_{25}	0.025	0.031	C_c	0.009	0.012
C_6	0.023	0.031	H_{26}	0.000	0.000	H_a	0.011	0.000
C_7	0.016	0.031	H_{27}	0.001	0.001	H_b	0.001	0.001
C_8	0.008	0.012	H_{28}	0.000	0.000	H_δ	absent	0.000
C_9	0.015	0.023	H_{29}	0.000	0.000	H_c	0.001	0.001
C_{10}	0.021	0.032	H_{30}	0.001	0.001			
C_{11}	0.022	0.034	H_{31}	0.000	0.000			
C_{12}	0.015	0.021	H_{32}	0.000	0.000			
C_{13}	0.010	0.013	H_{33}	0.001	0.001			
C_{14}	0.015	0.021	H_{34}	0.000	0.000			
C_{15}	0.022	0.034	H_{35}	0.000	0.000			
C_{16}	0.021	0.032	H_{36}	0.001	0.001			
C_{17}	0.015	0.023	H_{37}	0.000	0.000			
C_{18}	0.008	0.012	R_{38}[a]	0.169	0.311			
C_{19}	0.016	0.022	R_{39}[a]	0.001	absent			
C_{20}	0.023	0.031	R_{40}[a]	0.001	absent			

[a] R_{38} represents the fluorine atom and oxygen atom (of H_2O), respectively in F-Mb and Met-Mb. R_{39} and R_{40} are hydrogen atoms of H_2O in Met-Mb.

hemin derivatives. The corresponding amount is about 30% in the manganese derivatives, as is seen from Table II. This delocalization of the unpaired electronic spin population has been verified in the theoretical[5] and experimental studies[3] of the magnetic hyperfine interactions of ^{57}Fe and ^{14}N in the hemin derivatives and ^{55}Mn in the divalent compound studies. The drainage of the unpaired electronic spin population away from the central metal atom to the atoms in the porphyrin fifth and sixth ligands is expected to influence the magnetic hyperfine interactions of the protons in these molecules. From Table I it can be seen that there is a steady decrease in the unpaired electronic spin population on atoms in the metal–porphyrin unit and a consequent increase in this population on the halogen atoms[21] as we go from F–FeP to I–FeP. This transfer of the unpaired electronic population from the porphyrin ring to the fifth ligand in the halogen derivatives will be seen in section III to have significant influence on the meso proton hyperfine interactions in these molecules.

For the study of the hyperfine interactions of the proton with nuclear spin I one uses the spin-Hamiltonian[12]

$$\mathcal{H}_{spin} = A_c\mathbf{I}\cdot\mathbf{S} + \mathbf{I}\cdot\boldsymbol{B}\mathbf{S} \tag{6}$$

where S is the total electronic spin operator of the molecule, A_c is the Fermi contact coupling constant, and $\boldsymbol{B}$ is the dipolar hyperfine tensor for the nucleus. For the proton NMR shifts in solutions, one obtains[8] a contribution from A_c and also a residual contribution from $\boldsymbol{B}$ which arises from the anisotropic susceptibility of the molecule. ENDOR experiments,[3,11] where an external magnetic field is applied along the Z axis, provide the resultant hyperfine coupling constants $A_c + B_{zz}$. To evaluate A_c and B_{zz} theoretically one has to consider the electron-nuclear hyperfine Hamiltonian[12]

$$\mathcal{H}_{eN} = \frac{8\pi}{3}\gamma_e\gamma_H\hbar^2\mathbf{I}\cdot\sum_i \mathbf{s}_i\delta(\mathbf{r}_i) + \gamma_e\gamma_H\hbar^2\mathbf{I}\cdot\sum_i \frac{3\mathbf{r}_i(\mathbf{s}_i\cdot\mathbf{r}_i) - \mathbf{s}_i r_i^2}{r_i^5} \tag{7}$$

where γ_e and γ_H are the gyromagnetic ratios of the electron and the proton, and $\mathbf{s}_i$ and $\mathbf{r}_i$ the spin operator and the position vector (with respect to the proton) of the ith electron. The summation in both the terms in eq 7 is over all the electrons in the molecule. By equating the expectation value, over the electronic wave function for the molecules, of $\mathcal{H}_{spin}$ in eq 6 and $\mathcal{H}_{eN}$ in eq 7, one can obtain[12] expressions for the Fermi contact coupling constant A_c and the components of $\boldsymbol{B}$. Thus,

$$A_c = \frac{8\pi}{6S}\gamma_e\gamma_H\hbar^2\sum_\mu\{|\phi_\mu^\alpha(0)|^2 - |\phi_\mu^\beta(0)|^2\} \tag{8}$$

where the summation in eq 8 is over all the occupied MO's, S is the total spin of the molecule, and $|\phi_\mu(0)|^2$ represents the electronic density at the given proton site due to the μth MO. A_c can be expressed as the sum of two different contributions

$$A_c = A_d + A_{ex} \tag{9}$$

where the direct contribution

$$A_d = \frac{8\pi}{6S}\gamma_e\gamma_H\hbar^2\sum_{\substack{\mu \\ \text{unpaired}}}|\phi_{\mu(0)}|^2 \tag{10}$$

represents the interaction of the electrons in the unpaired MO's ϕ_μ with the nuclear moment. A_{ex} arises from the exchange interactions[12-15] between electrons in the unpaired MO's and those in the paired MO's. The evaluation of this contribution from first principles[15] is rather involved. However, the knowledge of the unpaired electronic population in various AO's in the molecule enables one to determine A_{ex} in a semiempirical manner.[14,15] The exchange interaction that arises between the unpaired electrons in the π orbital of an atom (meso carbon in case of meso proton) to which the H atom is bonded and the electrons in the σ bond between them (H and this adjacent atom) can be estimated by the semiempirical relation[14]

$$A_{ex}^\pi = \frac{Q^\pi}{2S}\rho^\pi \tag{11}$$

where ρ^π is the unpaired π-electron population of the adjacent atom and Q^π is a constant for a given fragment. For the CH fragment, which has been well investigated[13,14] both theoretically and experimentally, we have used a value of −70 MHz for Q^π. No such empirical value is available for Q^π in these cases to use in our present work. Theoretical investigations have been carried out in the past on the exchange polarization effect due to unpaired electrons in the $^2\Sigma$ and $^2\pi$ state of the OH radical,[15] the results of which suggest a value of −62.52 MHz for Q^π for the OH fragment. Since no such results are available for the NH fragment, we have used the mean value −66.26 MHz of the Q^π's for the CH and OH groups for this case. In addition to the exchange polarization produced by the unpaired π electrons, unpaired electrons in the σ orbitals can also exchange-polarize the paired electrons in the σ bond in the CH, NH, and OH fragments and

(21) This trend is in the opposite direction to that expected from simple electronegativity considerations for the net electronic populations on the halogen atoms, which has been found to be the case from the results of our calculations. The reason for this difference between the net electronic and unpaired spin population is that the latter arises from only the unpaired spin molecular orbitals.

Table IV. Dipolar Hyperfine Coupling Constants (MHz) of Meso Proton, Heme-Bound Protons, and Heme-Bound Water Proton

molecule	proton	B_{zz}^{M} [a]	B_{zz}^{A} [b]	$B_{zz}^{N+N'}$ [c]	B_{zz}^{rest} [c]	B_{zz}	B_{zz}^{loc}	B_{zz}^{A}/B_{zz}^{M}	B_{zz}^{loc}/B_{zz}
F-FeP	H_{27}	−0.505	−0.458	−0.206	−0.178	−1.347	−0.808	0.907	0.600
Cl-FeP	H_{27}	−0.524	−0.419	−0.195	−0.143	−1.281	−0.808	0.800	0.631
Br-FeP	H_{27}	−0.517	−0.332	−0.177	−0.121	−1.147	−0.808	0.623	0.704
I-FeP	H_{27}	−0.513	−0.308	−0.167	−0.104	−1.092	−0.808	0.600	0.740
OH-FeP	H_{27}	−0.500	−0.354	−0.161	−0.149	−1.164	−0.808	0.708	0.694
Met-Mb	H_{27}	−0.529	−0.105	−0.162	−0.155	−0.951	−0.836	0.198	0.879
	H_{30}	−0.529	−0.120	−0.163	−0.148	−0.960	−0.836	0.227	0.871
F-Mb	H_{27}	−0.509	−0.151	−0.190	−0.217	−1.067	−0.836	0.297	0.784
	H_{30}	−0.509	−0.162	−0.186	−0.218	−1.075	−0.836	0.318	0.778
H_2O-$Mn^{II}P$	H_{27}	−0.594	−0.243	−0.149	−0.177	−1.163	−0.831	0.409	0.715
	H_{30}	−0.594	−0.248	−0.149	−0.179	−1.170	−0.831	0.418	0.710
Cl-$Mn^{III}P$	H_{27}	−0.596	−0.299	−0.087	−0.159	−1.141	−0.831	0.384	0.728
OH-FeP	OH	4.334	23.951	0.270[d]	0.017	28.572	6.998	5.526	0.245
Met-Mb	H_2O	3.801	0.449	0.271	0.143	4.664	6.006	0.118	1.580
H_2O-$Mn^{II}P$	H_2O	5.077	0.399	0.235	0.077	5.788	7.102	0.079	1.227

[a] B_{zz}^{M} refers to the contribution from the unpaired spin on the metal atom (Fe or Mn). [b] B_{zz}^{A} refers to the contribution from the unpaired spin on the nearest atoms, e.g., meso carbon in meso proton. [c] $B_{zz}^{N+N'}$ and B_{zz}^{rest} refer to the contribution from the unpaired spin on the two nearest porphyrin nitrogens and the rest of the atoms, respectively. [d] This represents the contributions due to the unpaired spin on the four porphyrin nitrogens.

Table V. Dipolar Hyperfine Coupling Constants (in MHz) of Imidazole Protons in Met-Mb and F-Mb

molecule	proton	B_{zz}^{Fe} [a]	$B_{zz}^{N\epsilon}$ [b]	B_{zz}^{A}	$B_{zz}^{N+N'}$	B_{zz}^{rest}	B_{zz}	B_{zz}^{loc}	B_{zz}^{loc}/B_{zz}
Met-Mb	H_a	0.931	−0.297	−0.108	0.218	0.062	0.806	1.476	1.831
	H_c	1.131	−0.386	−0.075	0.246	0.352	1.268	1.787	1.409
F-Mb	H_a	0.896	−0.183	−0.079	0.261	0.104	0.999	1.471	1.472
	H_c	1.089	−0.183	−0.079	0.261	0.121	1.155	1.787	1.547
	H_δ	0.585	0.100	0.101	0.082	0.122	0.990	0.960	0.970

[a] B_{zz}^{Fe}, $B_{zz}^{N\epsilon}$, B_{zz}^{A}, $B_{zz}^{N+N'}$, and B_{zz}^{rest} refer to the contributions due to unpaired spins on the iron, the axial imidazole nitrogen, the nearest atom, the two nearest porphyrin nitrogens, and the rest of the atoms, respectively.

thus produce a hyperfine field at the proton. No empirical expressions are available for the study of this mechanism of exchange polarization; however, estimates for this type of exchange polarization effect can be made from the available results of calculation[15b] for the $^2\Sigma$ excited state of the OH radical. Such results show that the exchange polarization of the paired σ electrons in the OH radical by an unpaired σ electron leads to a positive exchange polarization contribution of about 63.0 MHz at the proton site, in contrast to the negative exchange polarization contribution by the unpaired π electrons in the $^2\pi$ ground state of the OH radical. In the absence of any available results for Q^σ for CH and NH, we use the same value as that for OH. Thus

$$A_{ex}^{\sigma} = \frac{Q^\sigma}{2S}\rho^\sigma \tag{12}$$

and the net A_{ex} in eq 9 is given by:

$$A_{ex} = A_{ex}^{\pi} + A_{ex}^{\sigma} \tag{13}$$

The third, and what will be seen from section III to be the major contribution to the proton hyperfine coupling constant, arises from the dipolar interaction[12] between the proton nuclear moment and the unpaired electrons distributed over the molecule. As has been mentioned earlier in this section, the components of the dipolar tensor $\boldsymbol{B}$ can be obtained by equating the expectation values of the dipolar part of $\mathcal{H}_{eN}$ in eq 7 to that of $\mathcal{H}_{spin}$ in eq 6 over the molecular wave functions. Since the hydrogen atom has only the 1s AO, there will not be any local contribution[5,17] to the dipolar hyperfine coupling constant arising from the AO of the hydrogen atom. It has often been the practice[11,14] in the literature to assume all the unpaired electrons to be localized at the metal atom and then use the classical point magnetic dipole approximation to determine the dipolar hyperfine field at the proton site. As is seen from Tables I, II, and III, this may not be appropriate since there is a great deal of delocalization of unpaired electronic spin in the molecules considered. We have used the better approximation of obtaining the components of the dipolar tensor from the point magnetic dipoles on all the different atoms as determined by the unpaired spin distribution over the molecule. For comparison with experimental results, where an external magnetic field is applied along the heme normal (Z axis), we need B_{zz}, which will be given by

$$B_{zz}(r_A) = \frac{g_Z\beta g_H\beta_N}{2S}\sum_{B>A}\rho_B\frac{3Z_{AB}^2 - r_{AB}^2}{r_{AB}^5} \tag{14}$$

with

$$r_{AB} = r_A - r_B$$

where β and β_N are the Bohr magneton and the nuclear magneton, respectively. g_Z is the g factor for the molecule along the heme normal and g_H that for the proton. The vector r_A is the position vector of the hydrogen atom under consideration and the r_B refer to the position vectors of other atoms in the molecule, ρ_B being the total unpaired electronic population on the atom B. In eq 14, the summation is carried out over all the atoms except the given hydrogen atom.

The above expression for B_{zz} is satisfactory when the distance between the given hydrogen atom and other atoms is large compared to the Bohr radius a_0 for the hydrogen atom. For the atom nearest to the given proton, the point dipole approximation might lead to some underestimation of the corresponding dipolar field. In this case, a better approximation is to use the expectation value of the dipolar Hamiltonian over the part of the unpaired electronic wave function residing on the nearest atom. We have made an estimation of this type in the case of meso proton and found it to give a contribution no more than 15% higher compared to the point dipole approximation for the nearest atom.

III. Results and Discussion

Our results for the various contributions to the proton hyperfine constants and their net values are presented in Tables IV–VII. We shall first consider the contributions individually and then the total hyperfine constants and their comparison with experiment.

A. Direct Contact Coupling Constant A_d. (i) Meso Proton. Considering the direct contact contribution A_d of the meso proton in the five-liganded compounds, we find for the ferric heme

Table VI. Hyperfine Coupling Constants (in MHz) of Protons in Five-Ligand High-Spin Hemin Derivatives

molecule	proton	A_d	A_{ex}	$A = A_d + A_{ex}$	B_{zz}	$A_H = A + B_{zz}$	A_H^{expt}
F-FeP	meso proton H_{27}	0.515	−0.483	0.033	−1.347	−1.314	0.951 ± 0.003
			−0.262	0.253		−1.094	
Cl-FeP		0.360	−0.446	−0.086	−1.281	−1.367	1.014 ± 0.003
			−0.281	0.079		−1.202	
Br-FeP		0.270	−0.356	−0.086	−1.147	−1.233	1.009 ± 0.005
			−0.231	0.039		−1.108	
I-FeP		0.210	−0.313	−0.103	−1.092	−1.195	
			−0.212	−0.002		−1.094	
OH-FeP	meso proton H_{27}	0.286	−0.373	−0.087	−1.164	−1.251	
			−0.259	0.027		−1.137	
	OH proton	8.438	−6.906	+1.532	28.572	29.104	
H_2O-$Mn^{II}P$	meso proton H_{27}	0.484	−0.238	0.246	−1.163	−0.917	
			−0.163	0.320		−0.843	
	H_{30}	0.469	−0.242	0.227	−1.170	−0.943	
			−0.163	0.306		−0.864	
	H_2O proton H_{39}	2.327	−1.416	0.911	5.788	6.699	
			−0.361	1.966		8.754	
Cl-$Mn^{III}P$	meso proton H_{27}	0.708	−0.283	0.425	−1.141	−0.716	
			−0.223	0.485		−0.656	

compounds a gradual decrease from the fluoro to the iodo derivatives (Table VI) in the halogen series as expected from the result seen from Table I that the unpaired electronic spin on the atoms in the metal porphyrin unit gradually decreases in this order. Although F, and OH groups are usually considered to be chemically similar, it is interesting to note that A_d in OH–FeP is much smaller than in F–FeP, a consequence of the result (Table I) that the unpaired electronic populations on the carbon atoms C_6, C_7, and C_8 (the facts of the atomic orbitals of which contribute to the spin density at the meso proton) are significantly different for OH–FeP and F–FeP. In the case of manganese porphyrins, A_d for the meso proton is seen from Table VI to be of the same order of magnitude as that in the five-liganded hemins. However, A_d in H_2O–$Mn^{II}P$ is much smaller than that in Cl–$Mn^{III}P$. This is due to the greater unpaired electron density at the meso proton from the d_{xy}-like MO in the trivalent manganese derivative than in the divalent one.

In Met–Mb and F–Mb, we have investigated all four meso protons H_{27}, H_{30}, H_{33}, and H_{36}. However, since H_{27} is nearly equivalent to H_{33} and H_{30} to H_{36}, we have presented results for only H_{27} and H_{30} in Table VI. The A_d for these meso protons is in the same range of values as discussed before for the five-liganded porphyrins, reflecting the comparable orders of the spin distributions in the metal–porphyrin unit for the two sets of systems (Tables I and II). Comparing A_d in F–FeP and F–Mb, it appears that binding of imidazole to iron increases the unpaired electron density at the meso proton, again reflecting the trend found in Table II for the unpaired spin populations for the carbon atoms C_6, C_7, and C_8 (and C_{12}, C_{13}, C_{14}) in the two compounds.

(ii) Metal-Bound OH and H_2O Protons. From Table VI, the A_d for the OH proton in OH–FeP is seen to be an order of magnitude larger than that for the meso protons, besides being the largest among all the protons studied. This happens mainly because of the large coefficients of H_{39}, O_{38}, and Fe atomic orbitals in the d_{z^2}-like unpaired molecular orbitals. The other factor is the smaller distance (2.7 Å) of the OH proton from Fe compared to a distance of about 4.5 Å in the case of meso protons. Metal-bound H_2O protons in H_2O–$Mn^{II}P$ and Met–Mb also have large values of A_d. The bent structure of M–O–H (M representing Fe or Mn) in Met–Mb and H_2O–$Mn^{II}P$, leading to weaker interaction between the d orbitals of Fe and the orbitals of the OH bonds of the H_2O molecule, explains the smaller value of A_d in these two molecules compared to that in OH–FeP where Fe–O–H is linear.

(iii) Imidazole Protons. There are three CH protons (Figure 2) namely H_a, H_b, and H_c in the imidazole of the model compound used for Met–Mb. An additional proton, namely the exchangeable proton H_δ (Figure 2), is present in the imidazole of the F–Mb. H_b belongs to a hypothetical atom replacing the rest of the histidine group besides imidazole in our model compound to reduce computational time. Also, in the real Met–Mb molecules, H_δ exchanges between N_δ (Figure 2) and the bulk water molecule. In our model compound for Met–Mb, H_δ was, however, absent since we wanted to use a neutral system. However, H_δ is present in our model compounds for F–Mb, and so we can make comparison with the experimental hyperfine constant for this exchangeable proton in F–Mb.

In both Met–Mb and F–Mb, A_d for H_c is seen from Table VII to be in general greater than that for H_a. This difference cannot be completely ascribed to the differences in the sixth axial ligand

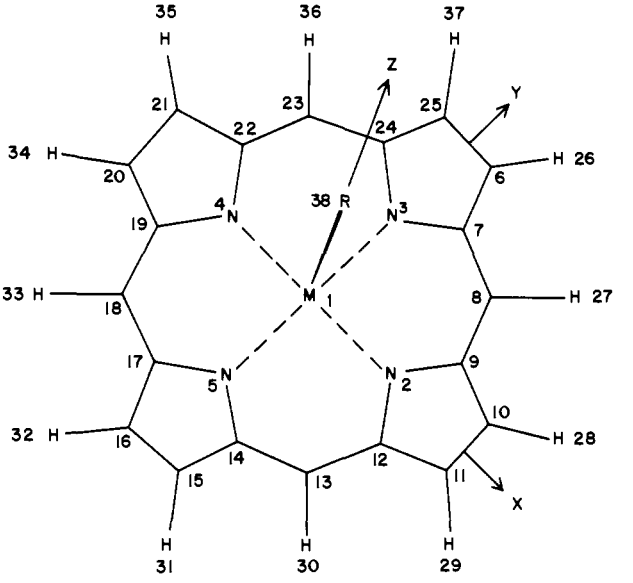

Figure 1. Atom or molecule with side chains replaced by protons. Atom or molecule ligates at R position for five-liganded systems under study.

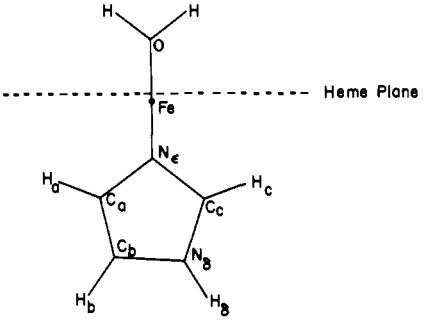

Figure 2. Structure of the model compound for Met–Mb. The planes containing H_2O and the imidazole are mutually perpendicular. H_δ is absent for the model compound for Met–Mb. In the case of the model compound for F–Mb, the sixth axial ligand is F⁻ in place of H_2O in Met–Mb.

Table VII. Hyperfine Coupling Constants (in MHz) of Protons in Met-Mb and F-Mb

molecule	proton	A_d	A_{ex}	A	B_{zz}	$A_H = A + B_{zz}$	A_H^{expt}
Met-Mb	meso proton H_{27}	0.498	−0.080	0.418	−0.951	−0.533	0.790
			0.045	0.543		−0.408	
	H_{30}	0.458	−0.097	0.361	−0.960	−0.599	
			0.065	0.523		−0.437	
	heme bound proton H_2O H_{31}	1.055	−0.972	0.083	4.664	4.747	6.0
			0.724	1.779		6.443	
	imidazole proton H_a	0.244	−0.126	0.118	0.806	0.924	
			0.082	0.326		1.132	
	H_c	0.541	−0.097	0.444	1.268	1.712	
			0.036	0.577		1.845	
F-Mb	meso proton H_{27}	0.619	−0.131	0.488	−1.068	−0.580	0.810
			0.087	0.706		−0.362	
	H_{30}	0.629	−0.138	0.491	−1.075	−0.584	
			0.075	0.704		−0.371	
	imidazole proton H_a	0.148	−0.015	0.133	0.999	1.132	
			0.075	0.152		1.151	
	H_δ	0.055	−0.091	−0.036	0.990	0.954	1.25 ± 0.03
			−0.073	−0.018		0.972	
	H_c	0.268	−0.152	0.116	1.155	1.271	
			−0.104	0.164		1.319	

since the structures of imidazole in the model systems used for these two molecules are also different, with the H_δ being absent in Met–Mb.

B. Exchange Polarization Coupling Constant A_{ex}. In analyzing the exchange polarization contributions to the proton hyperfine constants, we are faced with some ambiguity in defining π or σ characters for the unpaired spin molecular orbitals with respect to the paired spin–orbitals involving the hydrogen atom in question. Thus, considering the meso protons for example, we can consider the exchange polarization effect as arising from the three component 2p orbitals of the adjacent meso carbon. Of these, the 2p orbital perpendicular to the porphyrin plane can be clearly considered as π-like in treating the exchange polarization effect. For the other two 2p orbitals the characterization as being π- and σ-like is not as clearcut because the paired orbitals in which the hydrogen atom participates are not axially symmetric about the CH bond. We have therefore taken two extreme assumptions, one corresponding to both 2p orbitals perpendicular to the CH bond as π-like and the one along the CH bond as σ-like for exchange polarization effect and the other extreme involving only the 2p orbitals perpendicular to the porphyrin as π-like and the other two σ-like. Similar arguments apply to protons belonging to the NH bond. For the protons of the H_2O molecule in Met–Mb and H_2O–$Mn^{II}P$, the two extreme approximations correspond to either taking the oxygen 2p orbital along the Fe–O (or Mn–O) axis as π-like or σ-like for exchange polarization effects, the other 2p orbital in the plane of H_2O molecule being always considered as σ-like and that perpendicular to the H_2O plane as π-like. The two sets of entries for A_{ex} in Tables VI and VII refer to these extremes, with the actual situation being somewhere intermediate between the two. There is no such ambiguity for the OH proton since it is colinear with the Fe–O direction.

(i) **Meso Protons.** The trend of variation in A_{ex} among the five-liganded hemins is seen from Table VI to be similar to that in A_d discussed earlier. It is interesting to observe from Tables VI and VII that, because of the opposite sign and nearly comparable magnitudes of A_d and A_{ex}, there is a great deal of cancellation between these two in the five-liganded hemins. Consequently, the net contact coupling constants A_c for the meso protons have rather small magnitudes in these molecules, and the net hyperfine coupling constant will be mainly contributed to by the dipolar interaction (eq 14). In the case of the five-liganded manganese porphyrins, however, A_d is seen from Table VI to dominate over A_{ex}, leading to larger net contact contributions A as compared to the hemins.

In Met–Mb and F–Mb, A_{ex} is the smallest among all the meso protons. This is understandable in view of the decrease in the unpaired spin populations in the $2p_z$ orbitals of the meso carbons (Tables I and II) relative to the five-liganded systems, probably a consequence of movement of spin population toward the imidazole in the six-liganded systems. As a result of this decrease in magnitude of A_{ex}, A_c is seen to be larger in magnitude for the six-liganded system than that for the five-liganded counterparts.

(ii) **Metal-Bound OH and H_2O Protons.** From Table VI, A_{ex} is seen to have a very large negative value for the OH proton in OH–FeP, because a larger fraction (about 13%) of the total unpaired electronic spin population is in the π-like orbitals rather than in the σ-like orbitals of oxygen. Although A_{ex} values for the H_2O protons in H_2O–$Mn^{II}P$ and Met–Mb are seen from Tables VI and VII to be not as sizable as that in OH–FeP, they are still significantly larger in magnitude compared to A_{ex} for the meso protons. These large magnitudes (of opposite sign for the two extreme approximations explained earlier) are associated with the presence of substantially strong unpaired populations in the orbitals of oxygen atom (Tables I–III).

(iii) **Imidazole Protons.** As was the case for A_d, the A_{ex} for all the imidazole protons are seen from Table VII to be small. One cannot ascribe the differences between the A_{ex} for corresponding protons in Met–Mb and F–Mb to the differences in the sixth ligands F and H_2O, because of differences in the imidazoles in these two molecules as mentioned earlier in this section in discussing the A_d for these protons.

C. Dipolar Coupling Constants B_{zz}. The results for the dipolar hyperfine constants at the various protons, obtained using eq 14, are listed in Tables IV and V. For the purpose of obtaining an insight into the relative importance of the various sources contributing to the dipolar hyperfine constant, we have broken up the contributions into those arising from the unpaired spin populations on the metal atom, the nearest neighbor carbon, nitrogen or oxygen atom adjacent to the proton in question, and from the rest of the atoms in the molecules. The results show that, other than one or two exceptions, the contributions from the metal and nearest neighbor atoms are comparable, the rest of the atoms also having a significant influence on the net dipolar hyperfine constant.

As mentioned earlier, in section II, the approximation has often been made[10,13,21] in the literature that for molecules containing paramagnetic metal atoms, the dipolar fields at the protons could be approximated by assuming the entire unpaired spin population to be localized on the metal atom. Therefore, we have listed in Tables IV and V the dipolar hyperfine constants in this localized approximation to compare with the net dipolar hyperfine results. This comparison shows that overall there are substantial differences between the two results, the localized approximation[10,13] leading to significant underestimation in the magnitude of the dipolar field in most cases and overestimation in a few.

(i) **Meso Protons.** For the meso protons in all the five-liganded compounds (Table IV), including both the divalent and trivalent manganese compounds, the leading contribution (B_{zz}^M) arises from the unpaired spin population on the metal atom. Substantial contributions also arise from the unpaired spin populations on the

nearest neighbor carbon atom (B_{zz}^{A}), the nearest two pyrrole nitrogen atoms ($B_{zz}^{N+N'}$), and the rest of the atoms (B_{zz}^{rest}) in the molecules. The order of importance of these latter three contributions for the case of the five-liganded heme compounds is in the order they are stated, while for the manganese compounds, the order of $B_{zz}^{N+N'}$ and B_{zz}^{rest} is reversed, reflecting a difference in the details of the spin distribution over these two sets of compounds. For the six-liganded systems Met–Mb and F–Mb, the dipolar contributions to B_{zz}^{M} are seen from Table IV to be comparable to those for the five-liganded compounds, as expected from the similar spin populations on the iron atom as seen from Tables I and III. However, there is an important relative change in the order of the other contributions, B_{zz}^{A} now appearing to be somewhat smaller than $B_{zz}^{N+N'}$ and B_{zz}^{rest} the reduction of B_{zz}^{A} being a result of the decrease in unpaired spin population on C-8 owing to the competition for this population by the imidazole ligand in the six-liganded compounds.

The magnitudes of the total B_{zz} at the meso protons in all the five- and six-liganded systems are seen from Table IV to be reasonably close to each other, with those for the six-lianded system somewhat smaller because of the smaller sizes of the B_{zz}^{A} in the latter cases. The importance of the delocalized nature of the spin distribution with substantial drainage of unpaired spin population from the metal atoms to the ligands is evidenced by the values of the ratio B_{zz}^{A}/B_{zz} which ranges from 0.9 for fluorohemin to about 0.2 for Met–Mb. The localized approximation often used[11,21] assuming all the unpaired spin population to be on the metal atom is seen to be not a good approximation from both the unpaired spin populations on the various atoms listed in Table I, and also the comparable sizes of B_{zz}^{M} and the sum of B_{zz}^{A}, $B_{zz}^{N+N'}$, and B_{zz}^{rest}. This substantial departure from the localized spin model is also illustrated by the departure from unit of B_{zz}^{loc}/B_{zz} for the various molecules in the last column of Table IV, this ratio ranging from 0.6 for the meso protons in fluorohemin to 0.88 in Met–Mb.

(ii) Metal-Bound OH and H_2O Protons. Considering first the protons on the H_2O molecules attached to iron and manganese atoms, we find from Table IV that the dipolar contributions to the hyperfine constants from the spin populations on the metal atom are substantially larger and of opposite sign as compared to the meso protons. This can be understood by noting (section II) that the protons on the H_2O ligand are much closer to the metal atom than the meso protons and are also disposed at polar angles θ with respect to the Z axis smaller than the magic angle 54° 36′ after which $(3\cos^2\theta - 1)$ becomes negative, while for the line joining the meso proton to the metal atom, θ is close to 90°. The contributions from the spin populations on the oxygen atom, the porphyrin nitrogen atoms, and the rest of the atoms in the molecule are, on the other hand, more comparable in nature to those for the meso protons since the distances from these atoms to the water protons and meso protons are quite similar. As a consequence of these two features, the ratios of B_{zz}^{A}/B_{zz}^{M} for the water protons are significantly smaller than for the meso protons. For the proton in the OH group in hematin, the dominant contributor is the unpaired spin population at the oxygen site which is significantly larger than that in Met–Mb and H_2O–$Mn^{II}P$ (Tables II and III), making B_{zz}^{A} more than five times larger than B_{zz}^{M}, the metal atom contribution. As far as the validity of the local approximation of taking all five unpaired spins to be located on the metal atom is concerned, the ratios B_{zz}^{loc}/B_{zz} for the OH and water protons are again seen to be indicative of very significant departures from the local approximation, the ratio for hematin being about 0.25, considerably smaller than unity, while for the water protons the ratios are substantially larger than unity. This difference in the nature of the departure from the local approximation for the OH and water protons is again a reflection of the different relative importance of B_{zz}^{M} and B_{zz}^{A} for these two types of protons.

(iii) Imidazole Protons. The features of the dipolar hyperfine constants for the imidazole protons in Table V are best described by comparing them with meso protons. Thus the B_{zz}^{M} for H_a and H_c protons in Met–Mb and F–Mb are about twice as large and of opposite sign to those for meso protons, a consequence of shorter distances to the metal atom as compared to the latter and polar angle smaller than the magic angle. The net B_{zz}'s, however, are comparable to those for meso protons, because of the interesting fact that while there is now substantial cancellation among the rest of the contributions $B_{zz}^{N_\delta}$, B_{zz}^{A}, $B_{zz}^{N+N'}$, and B_{zz}^{rest}, the corresponding contributions for the meso protons were all of the same sign, again a consequence of polar angle considerations. The same polar angle considerations are responsible for the fact that all the dipolar contributions for H_δ have positive signs and add up to a net B_{zz} comparable to H_a and H_b.

It is interesting also to note from Table VII that the percentage differences in B_{zz} between the Met–Mb and F–Mb are significantly smaller than in A_{ex}. This is because while A_{ex} derives its contribution from mainly the unpaired spin population on the nearest neighbor atoms, which can have significant differences between the two molecules, B_{zz} is more long range and is more reflective of the overall unpaired spin population distribution in the two molecules which tend to be more similar.

Finally, the ratios B_{zz}^{loc}/B_{zz} in the cases of H_a and H_c are again seen from Table V to show important departures from the localized model, in the same direction as for the water protons in Met–Mb and H_2O–$Mn^{II}P$ (Table IV), B_{zz}^{loc} giving an overestimation. For H_δ, the ratio B_{zz}^{loc}/B_{zz} is fortuitously close to unity, although the unpaired spin population distributions on the atoms are considerably delocalized, both as seen from Table III and from the comparable magnitudes of B_{zz}^{M} and the sum of the contributions from the rest of the atoms.

D. Total Hyperfine Constants: Comparison with Experiment. Returning to Tables VI and VII, we have the net values of B_{zz} listed alongside the direct and exchange contributions, as well as the total hyperfine constants and the experimental results wherever available. In general, it appears from the tables that, whereas the dipolar contribution B_{zz} is the dominant one, A_d and A_{ex} are by no means unimportant. However, except in a few cases, there is substantial cancellation between A_d and A_{ex} which have opposite sign, making the magnitudes of their sum significantly smaller than their individual magnitudes. The major importance of the dipolar contributions to the hyperfine fields at proton sites is in contrast to the situations for the ^{57}Fe and ^{14}N nuclei and is a result of the fact that the protons are in the peripheral regions of the molecules, in contrast to the central region where the spin densities at the nuclei are substantially stronger, leading to the predominance of direct and exchange contributions. Experimental data on the net hyperfine constants at the protons are unfortunately available only in a few systems, and, from Tables VI and VII, it is seen that for these cases there is overall good agreement with theory. We proceed next to the discussion of the features of the total hyperfine constant results for the three classes of protons we have studied.

(i) Meso Protons. The meso protons are seen from Tables VI and VII to fall into two categories in terms of the relative importance of $A_d + A_{ex}$ and B_{zz}. Thus, for the cases of the five-liganded heme compounds with halogen and hydroxyl ligands, there is significant cancellation between A_d and A_{ex}, making the net hyperfine constants close to B_{zz}. In contrast, for Met–Mb, F–Mb, and Cl–$Mn^{III}P$, there is lesser cancellation between A_d and A_{ex}, the sum of A_d and A_{ex} being quite substantial compared to B_{zz} and of opposite sign, leading to total hyperfine constants small compared to B_{zz}. As regards comparison with experiment,[10] for the cases of hemin and its fluoro and bromo derivatives, there is satisfactory overall agreement with experiment both with respect to magnitudes and the trend of comparable hyperfine constants in the three. In the case of the six-liganded compounds F–Mb and Met–Mb (Table VII), the agreement with experiment[11] is not as good as in the case of the five-liganded systems for the absolute magnitudes, but the experimental trends such as comparable hyperfine constants in both these compounds and their smaller sizes with respect to the five-liganded systems are explained by our theoretical results. It is interesting that, of the two choices for A_{ex}, the first one leads to better agreement with theory for the six-liganded systems, while the opposite is the case for the five-liganded systems, indicating that the proper value of A_{ex} lies between the two extremes.

(ii) H_2O and OH Protons. Considering first the proton in the OH group in OH–FeP, the model compound for hematin, the dipolar interaction is seen from Table VI to be the dominant contributor to the hyperfine field. The direct contribution A_d is also sizable, because as mentioned earlier, the d_{z^2}-like molecular orbital has significant density at the proton site. However, it is cancelled substantially by A_{ex} from the π-like (with respect to the OH bond) spin density on the oxygen atom. The net hyperfine field on the OH proton of hematin is the largest of all the protons in all the systems we have analyzed. From our experience regarding the relationship of results for fluoromyoglobin and fluorohemin, we expect from analogy with hematin that the proton hyperfine constant in hydroxymyoglobin would also be sizable.

As regards the water protons, in both H_2O–$Mn^{II}P$ and Met–Mb, the net hyperfine constants (Tables VI and VII) are sizable, relatively large compared to the meso protons, but considerably smaller than for the OH proton in hematin. For both the H_2O-containing systems, the dipolar contribution is seen to be the leading one, but A_d and A_{ex} also make important contribution to the total hyperfine constant, A_H. The experimental value of A_H is available only for Met–Mb and is seen to lie between the theoretical values for the two choices of A_{ex}, again indicating that the actual values of A_{ex} would lie between the two choices. It is also gratifying that experimental[11] data in Met–Mb (Table VII) verify the theoretical result of the net hyperfine constant for water proton being an order of magnitude larger than for the meso proton.

(iii) Imidazole Protons. With respect to the relative sizes of the dipolar contribution B_{zz} and the isotropic contribution $A_d + A_{ex}$, the imidazole protons are seen from Table VII to fall into two categories. For the H_a and H_b protons, while the dipolar contribution is the major one, the isotropic effects also makes a significant net contribution. On the other hand, for H_δ, both A_d and A_{ex} are small, making B_{zz} the dominant contributor. Of the three types of proximal imidazole protons, experimental data are available only for H_δ in both F–Mb and Met–Mb. As mentioned earlier, our model compound for Met–Mb does not have an H_δ in this compound. For F–Mb, however, the experimental value is seen to be in good agreement with theory. It is also satisfying that the theoretical and experimental results[11] both have the trend that the H_δ hyperfine constant in F–Mb and Met–Mb is substantially smaller than that for the water protons in Met–Mb.

IV. Conclusion

One of the main features of our results is that the dipolar effect makes a major contribution to the hyperfine fields at the protons in high-spin heme and hemoglobin systems. Further, our analysis shows that it is important in this respect to consider the actual unpaired spin population distribution over the entire molecule in question, instead of making the commonly used approximation[10,13,22] of taking all the unpaired spin population as localized on the central metal atom. Also the direct and exchange contact contributions, while usually smaller than the dipolar in magnitude, have to be considered carefully because they have an important influence on the net hyperfine constant, either because in some instances they combine to make significant contributions or in others because they nearly cancel each other. For a number of the protons that we have considered and where experimental data are available, the experimental trend of variation among different protons is well reproduced by them, and also satisfactory agreement between theory and experiment is found for the actual magnitude of the hyperfine constants for individual protons. It would be helpful to have further experimental results to check the calculated hyperfine constants for a number of the protons where data are not currently available. However, from the satisfactory agreement between theoretical and experimental hyperfine constants for the variety of protons where data are already available, one can conclude that the unpaired spin populations that have been obtained in the present work give a reasonably accurate description of the true state of affairs in the peripheral regions of heme and hemoglobin systems, complementing similar conclusions found[5,6] for the more central regions of these systems from the analysis of ^{57}Fe and ^{14}N hyperfine fields.

Acknowledgment. The authors are grateful to Professor Charles P. Scholes for valuable discussions and suggestions.

(22) H. M. McConnell and J. Strathdee, *Mol. Phys.*, **2**, 129 (1959).

Gas-Phase Chemiionization Reactions of Antimony Pentafluoride

L. Lee, J. A. Russell, R. T. M. Su,† R. J. Cross, and M. Saunders*

Contribution from the Chemistry Department, Yale University, Box 6666, New Haven, Connecticut 06511. *Received March 17, 1981*

Abstract: Using crossed molecular beams, we have studied the reactions of SbF_5 and its polymers with organic halides (RX). Monomer SbF_5 reacts with some RX species to produce $R^+ + SbF_5X^-$. Dimer reacts with a wider variety of RX species to produce $R^+ + SbF_6^- + SbF_4X$. Unless R^+ is particularly subject to cleavage, only the parent R^+ is observed; this indicates that the product is formed with only a small amount of internal energy.

It has recently become possible to study, in the gas phase, well-known solution reactions and thereby learn about the effects of solvent.[1] Studies of ion–molecule reactions with use of ICR show that differences in solvation energy between the reactants, the transition state, and the products can make large differences in the rate and thermochemistry of reactions in the gas phase and in solution. We report here the results of a gas-phase study of a chemiionization reaction which is well-known in solution,[2]

$$SbF_5 + RX \rightarrow SbF_5X^- + R^+ \quad (1)$$

Reaction 1 is commonly used to prepare stable solutions of carbonium ions for structural analysis by NMR or for further reaction. The reaction may be viewed as a halide abstraction by the extremely strong Lewis acid SbF_5. It occurs rapidly and irreversibly in solution for tertiary and secondary halides. The

† Department of Chemistry, National Taiwan University, Taipei, Taiwan, Republic of China.

(1) R. T. McIvers, *Sci. Am.*, **243** (No. 5), 186 (1980). J. L. Beauchamp, *Ann. Rev. Phys. Chem.*, **22**, 527 (1971).

(2) G. A. Olah, E. B. Baker, J. C. Evans, W. S. Tolgyesi, J. S. McIntyre, and I. J. Bastien, *J. Am. Chem. Soc.*, **86**, 1360 (1964). G. A. Olah, W. S. Tolgyesi, S. J. Kuhn, M. E. Moffatt, I. J. Bastien, and E. B. Baker, *J. Am. Chem. Soc.*, **85**, 1328 (1963). M. Saunders, P. Vogel, E. L. Hagen, and J. Rosenfeld, *Acc. Chem. Res.*, **6**, 53 (1973).

0002-7863/81/1503-5031$01.25/0